

Lanthanide(III) and Actinide(III) Complexes $[M(\text{BH}_4)_2(\text{THF})_5][\text{BPh}_4]$ and $[M(\text{BH}_4)_2(18\text{-crown-6})][\text{BPh}_4]$ ($M = \text{Nd, Ce, U}$): Synthesis, Crystal Structure, and Density Functional Theory Investigation of the Covalent Contribution to Metal-Borohydride Bonding

Thérèse Arliguie,[†] Lotfi Belkhir,[‡] Salah-Eddine Bouaoud,[‡] Pierre Thuéry,[†] Claude Villiers,[†] Abdou Boucekine,^{*,§} and Michel Ephritikhine^{*,†}

CEA, IRAMIS, Service de Chimie Moléculaire, CNRS URA 331, CEA/Saclay, 91191 Gif-sur-Yvette, France, Laboratoire de Chimie Moléculaire (LACMOM), Département de Chimie, Faculté des Sciences, Université Mentouri de Constantine, BP 325, Route de l'Aéroport Ain El Bey, 25017 Constantine, Algeria, and UMR CNRS 6226 Sciences Chimiques de Rennes, Université de Rennes 1, Campus de Beaulieu, 35042 Rennes, France

Received September 2, 2008

Treatment of $[M(\text{BH}_4)_3(\text{THF})_3]$ with $\text{NEt}_3\text{HBPh}_4$ in THF afforded the cationic complexes $[M(\text{BH}_4)_2(\text{THF})_5][\text{BPh}_4]$ [$M = \text{U}$ (**1**), Nd (**2**), Ce (**3**)] which were transformed into $[M(\text{BH}_4)_2(18\text{-crown-6})][\text{BPh}_4]$ [$M = \text{U}$ (**4**), Nd (**5**), Ce (**6**)] in the presence of 18-crown-6; $[\text{U}(\text{BH}_4)_2(18\text{-thiacrown-6})][\text{BPh}_4]$ (**7**) was obtained from **1** and 18-thiacrown-6 in tetrahydrothiophene. Compounds **1**, **3** · $\text{C}_4\text{H}_8\text{S}$, **4** · THF, **5**, and **6** · THF exhibit a penta- or hexagonal bipyramidal crystal structure with the two terdentate borohydride ligands in apical positions; the BH_4 groups in the crystals of **7** · $\text{C}_4\text{H}_8\text{S}$ are in relative *cis* positions, and the thiacycrown-ether presents a saddle shape, with two diametrically opposite sulfur atoms bound to uranium in *trans* positions. The crystal structures of these complexes, as well as those of previously reported $[M(\text{BH}_4)_2(\text{THF})_5]^+$ cations, do not reveal any clear-cut lanthanide(III)/actinide(III) differentiation. The structural data obtained for $[M(\text{BH}_4)_2(18\text{-crown-6})]^+$ ($M = \text{U, Ce}$) by relativistic density functional theory (DFT) calculations are indicative of a small shortening of the $\text{U} \cdots \text{B}$ with respect to the $\text{Ce} \cdots \text{B}$ distance, which is accompanied by a lengthening of the $\text{U}-\text{H}_b$ bonds and an opening of the $\text{H}_b-\text{B}-\text{H}_b$ angle ($\text{H}_b =$ bridging hydrogen atom of the $\eta^3\text{-BH}_4$ ligand). The Mulliken population analysis and the natural bond orbital analysis indicate that the $\text{BH}_4 \rightarrow \text{M(III)}$ donation is greater for $M = \text{U}$ than for $M = \text{Ce}$, as well as the overlap population of the $\text{M}-\text{H}_b$ bond, thus showing a better interaction between the uranium 5f orbitals and the H_b atoms. The more covalent character of the $\text{B}-\text{H}-\text{U}$ three-center two-electron bond was confirmed by the molecular orbital (MO) analysis. Three MOs represent the π bonding interactions between U(III) and the three H_b atoms with significant 6d and 5f orbital contributions. These MOs in the cerium(III) complex exhibit a much lesser metallic weight with practically no participation of the 4f orbitals.

Introduction

Borohydride complexes of the f-elements are generally more stable than those of the d transition metals and are interesting for studying the structural properties and chemical behavior of the BH_4 ligand.¹ The nature of the metal-

borohydride bonds in these complexes is a subject of much debate. These bonds were considered as mostly ionic, in view of the high coordination numbers, complying with the principle of maximum occupancy of the coordination sphere and the clear-cut fluxionality of the BH_4 ligands. The similarity of the structural and dynamic properties of the borohydride complexes of the f-elements and those with central d^0 ions led to the conclusion that f electrons do not participate in the formation of the $\text{M}-\text{BH}_4$ bonds. Otherwise, the covalent character of these compounds, suggested by their

* To whom correspondence should be addressed. E-mail: abdou.boucekine@univ-rennes1.fr (A.B.), michel.ephritikhine@cea.fr (M.E.).

[†] CEA/Saclay.

[‡] Université Mentouri de Constantine.

[§] CNRS-Université de Rennes 1.

high volatility and solubility in nonpolar solvents, was related to the covalent nature of the B–H–M three-center two-electron bridging bond. According to the isolobality concept, the borohydride ligand with η^1 , η^2 , or η^3 denticity is closely analogous to the chloride, allyl, or cyclopentadienyl anion, respectively.²

The uranium borohydrides $U(BH_4)_4$,³ $[U(BH_4)_3(C_6Me_6)]$,⁴ and, more recently, the lanthanide borohydrides $[Ln(BH_4)_3(THF)_3]$,⁵ proved to be valuable precursors to inorganic and organometallic derivatives resulting from reactions of the BH_4 groups with anionic reagents or proton acidic substrates. Protonolysis of the M– BH_4 bond with acidic ammonium salts was devised as a convenient route to cationic complexes, as shown by the synthesis of $[U(BH_4)_2(THF)_5][BPh_4]$ (**1**) from $[U(BH_4)_3(THF)_3]$.⁶ In view of the often remarkable performances of cationic complexes in catalysis, the lanthanide counterparts of **1**, $[Ln(BH_4)_2(THF)_5][BPh_4]$ ($Ln = Y, Sm, Nd, La$), were very recently isolated from the protonolysis reaction of $[Ln(BH_4)_3(THF)_3]$ and were found to efficiently activate the ring-opening polymerization of ϵ -caprolactone.⁷ Similarly, $[Nd(BH_4)_2(THF)_5][B(C_6F_5)_4]$ was synthesized by protonolysis of $[Nd(BH_4)_3(THF)_3]$ with $[NMe_2PhH][B(C_6F_5)_4]$ and was found to be an efficient precatalyst for isoprene polymerization.⁸

Comparison of the crystal structures of a variety of isomorphous and/or isostructural trivalent lanthanide and uranium complexes showed that, allowing for the variation in the ionic radii of the metals, the bonds between the 5f-element and the soft and/or π -accepting ligands are shorter

than the corresponding bonds in the lanthanide analogues.^{9,10} This shortening is explained by a modest enhancement of covalence in the actinide versus lanthanide–ligand bonding, a difference which plays an essential role in the selective complexation of trivalent 5f over 4f ions, finding a particular application in the reprocessing of spent nuclear fuel.¹¹ Since the bonds between the BH_4 ligand and d transition metals or f-elements are generally considered to have a significant degree of covalent character, it was appealing to determine if, and by what amount, this feature would be more pronounced in the uranium than in the lanthanide complexes. We present herein the synthesis and characterization of the uranium compound $[U(BH_4)_2(THF)_5][BPh_4]$ (**1**) and its neodymium (**2**) and cerium (**3**) counterparts, including the crystal structure of **3**· C_4H_8S ; we also describe the synthesis and crystal structures of the crown-ether derivatives $[M(BH_4)_2(18\text{-crown-6})][BPh_4]$ [$M = U$ (**4**), Nd (**5**), Ce (**6**)], and $[U(BH_4)_2(18\text{-thiacrown-6})][BPh_4]$ (**7**) (18-thiacrown-6 = 1,4,7,10,13,16-hexathiacyclooctadecane). Finally, we make use of relativistic density functional theory (DFT) to study the electronic structure of **4** and **6**, to give, for the first time, a clear insight into the covalent contribution to the metal–borohydride bond.

Experimental Section

All reactions were carried out under argon (<5 ppm oxygen or water) using standard Schlenk-vessel and vacuum line techniques or in a glovebox. Solvents were dried by standard methods and

- (9) (a) Iveson, P. B.; Rivière, C.; Guillauneux, D.; Nierlich, M.; Thuéry, P.; Ephritikhine, M.; Madic, C. *Chem. Commun.* **2001**, 1512. (b) Rivière, C.; Nierlich, M.; Ephritikhine, M.; Madic, C. *Inorg. Chem.* **2001**, *40*, 4428. (c) Berthet, J. C.; Rivière, C.; Miquel, Y.; Nierlich, M.; Madic, C.; Ephritikhine, M. *Eur. J. Inorg. Chem.* **2002**, 1439. (d) Berthet, J. C.; Miquel, Y.; Iveson, P. B.; Nierlich, M.; Thuéry, P.; Madic, C.; Ephritikhine, M. *J. Chem. Soc., Dalton Trans.* **2002**, 3265. (e) Cendrowski-Guillaume, S. M.; Le Gland, G.; Nierlich, M.; Ephritikhine, M. *Eur. J. Inorg. Chem.* **2003**, 1388. (f) Berthet, J. C.; Nierlich, M.; Ephritikhine, M. *Polyhedron* **2003**, *22*, 3475. (g) Mehdoui, T.; Berthet, J. C.; Thuéry, P.; Ephritikhine, M. *Dalton Trans.* **2004**, 579. (h) Mehdoui, T.; Berthet, J. C.; Thuéry, P.; Ephritikhine, M. *Eur. J. Inorg. Chem.* **2004**, 1996. (i) Mehdoui, T.; Berthet, J. C.; Thuéry, P.; Ephritikhine, M. *Dalton Trans.* **2005**, 1263. (j) J. C. Berthet, J. C.; M. Nierlich, M.; Y. Miquel, Y.; C. Madic, C.; M. Ephritikhine, M. *Dalton Trans.* **2005**, 369. (k) Mehdoui, T.; Berthet, J. C.; Thuéry, P.; Salmon, L.; Rivière, E.; Ephritikhine, M. *Chem.—Eur. J.* **2005**, *11*, 6994. (l) Roger, M.; Belkhir, L.; Thuéry, P.; Arliquie, T.; Fourmigué, M.; Boueckine, A.; Ephritikhine, M. *Organometallics* **2005**, *24*, 4940. (m) Roger, M.; Barros, N.; Arliquie, T.; Thuéry, P.; Maron, L.; Ephritikhine, M. *J. Am. Chem. Soc.* **2006**, *128*, 8790. (n) Roger, M.; Belkhir, L.; Arliquie, T.; Thuéry, P.; Boueckine, A.; Ephritikhine, M. *Organometallics* **2008**, *27*, 33.
- (10) (a) Brennan, J. G.; Stults, S. D.; Andersen, R. A.; Zalkin, A. *Organometallics* **1988**, *7*, 1329. (b) Wietzke, R.; Mazzanti, M.; Latour, J. M.; Pécaut, J. *Inorg. Chem.* **1999**, *38*, 3581. (c) Wietzke, R.; Mazzanti, M.; Latour, J. M.; Pécaut, J. *J. Chem. Soc., Dalton Trans.* **2000**, 4167. (d) Mazzanti, M.; Wietzke, R.; Pécaut, J.; Latour, J. M.; Maldivi, P.; Remy, M. *Inorg. Chem.* **2002**, *41*, 2389. (e) Karmazin, L.; Mazzanti, M.; Pécaut, J. *Chem. Commun.* **2002**, 654. (f) Karmazin, L.; Mazzanti, M.; Bezombes, J. P.; Gateau, C.; Pécaut, J. *Inorg. Chem.* **2004**, *43*, 5147. (g) Guillaumont, D. *J. Phys. Chem. A* **2004**, *108*, 6893.
- (11) (a) Nash, K. L. *Solvent Extr. Ion Exch.* **1993**, *11*, 729. (b) Nash, K. L. Separation chemistry for lanthanides and trivalent actinides. In *Handbook on the physics and chemistry of rare earths*; Gschneidner, K. A., Jr., Eyring, L., Choppin, G. R., Lander, G. H., Eds.; Elsevier Science: New York, 1994; Vol. 18 (121), p 197. (c) *Actinides and Fission Products Partitioning and Transmutation. Status and Assessment Report*, NEA/OECD Report; NEA/OECD: Paris, 1999. (d) *Implications of Partitioning and Transmutation in Radioactive Waste Management*; IAEA - TRS 435; IAEA: Vienna, Austria, 2005.
- (1) (a) Marks, T. J.; Kolb, J. R. *Chem. Rev.* **1977**, *77*, 263. (b) Xu, Z.; Lin, Z. *Coord. Chem. Rev.* **1996**, *156*, 139. (c) Ephritikhine, M. *Chem. Rev.* **1997**, *97*, 2193. (d) Makhaev, V. D. *Russ. Chem. Rev.* **2000**, *69*, 727.
- (2) Mancini, M.; Bougeard, P.; Burns, R. C.; Mlekuz, M.; Sayer, B. G.; Thompson, J. I. A.; McGlinchey, M. J. *Inorg. Chem.* **1984**, *23*, 1072.
- (3) (a) Baudry, D.; Charpin, P.; Ephritikhine, M.; Folcher, G.; Lambard, J.; Lance, M.; Nierlich, M.; Vigner, J. *J. Chem. Soc., Chem. Commun.* **1985**, 1553. (b) Baudry, D.; Bulot, E.; Ephritikhine, M. *J. Chem. Soc., Chem. Commun.* **1988**, 1369. (c) Baudry, D.; Bulot, E.; Charpin, P.; Ephritikhine, M.; Lance, M.; Nierlich, M.; Vigner, J. *J. Organomet. Chem.* **1989**, *371*, 163. (d) Baudry, D.; Bulot, E.; Ephritikhine, M.; Nierlich, M.; Lance, M.; Vigner, J. *J. Organomet. Chem.* **1990**, *388*, 279. (e) Baudry, D.; Bulot, E.; Ephritikhine, M. *J. Organomet. Chem.* **1990**, *397*, 169. (f) Gradoz, P.; Baudry, D.; Ephritikhine, M.; Nief, F.; Mathey, F. *J. Chem. Soc., Dalton Trans.* **1992**, 3047. (g) Leverd, P. C.; Lance, M.; Nierlich, M.; Vigner, J.; Ephritikhine, M. *J. Chem. Soc., Dalton Trans.* **1993**, 2251. (h) Leverd, P. C.; Lance, M.; Vigner, J.; Nierlich, M.; Ephritikhine, M. *J. Chem. Soc., Dalton Trans.* **1995**, 237.
- (4) (a) Baudry, D.; Bulot, E.; Charpin, P.; Ephritikhine, M.; Lance, M.; Nierlich, M.; Vigner, J. *J. Organomet. Chem.* **1989**, *371*, 155. (b) Baudry, B.; Bulot, E.; Ephritikhine, M. *J. Chem. Soc., Chem. Commun.* **1988**, 1316. (c) Baudry, D.; Ephritikhine, M.; Nief, F.; Ricard, L.; Mathey, F. *Angew. Chem., Int. Ed. Engl.* **1990**, *29*, 1485.
- (5) (a) Arliquie, T.; Lance, M.; Nierlich, M.; Ephritikhine, M. *J. Chem. Soc., Dalton Trans.* **1997**, 2501. (b) Cendrowski-Guillaume, S. M.; Nierlich, M.; Lance, M.; Ephritikhine, M. *Organometallics* **1998**, *17*, 786. (c) Cendrowski-Guillaume, S. M.; Le Gland, G.; Nierlich, M.; Ephritikhine, M. *Organometallics* **2000**, *19*, 5654. (d) Arliquie, T.; Doux, M.; Mézailles, N.; Thuéry, P.; Le Floch, P.; Ephritikhine, M. *Inorg. Chem.* **2006**, *45*, 9907. (e) Roger, M.; Arliquie, T.; Thuéry, P.; Ephritikhine, M. *Inorg. Chem.* **2008**, *47*, 3863.
- (6) Arliquie, T.; Lance, M.; Nierlich, M.; Vigner, J.; Ephritikhine, M. *J. Chem. Soc., Chem. Commun.* **1994**, 847.
- (7) Robert, D.; Kondracka, M.; Okuda, J. *Dalton Trans.* **2008**, 2667.
- (8) Visseaux, M.; Mainil, M.; Terrier, M.; Mortreux, A.; Roussel, P.; Mathivet, T.; Destarac, M. *Dalton Trans.* **2008**, 4558.

Table 1. Crystal Data and Structure Refinement Details

	1	3 ·C ₄ H ₈ S	4 ·THF	5	6 ·THF	7 ·C ₄ H ₈ S
chemical formula	C ₄₄ H ₆₈ B ₃ O ₅ U	C ₄₈ H ₇₆ B ₃ O ₅ Sc	C ₄₀ H ₆₀ B ₃ O ₇ U	C ₃₆ H ₅₂ B ₃ O ₆ Nd	C ₄₀ H ₆₀ B ₃ O ₇ Ce	C ₄₀ H ₆₀ B ₃ S ₇ U
<i>M</i> /g mol ⁻¹	947.44	937.70	923.34	757.45	825.43	1035.76
crystal system	orthorhombic	triclinic	triclinic	monoclinic	triclinic	monoclinic
space group	<i>Pbca</i>	<i>P</i> $\bar{1}$	<i>P</i> $\bar{1}$	<i>P</i> ₂ / <i>n</i>	<i>P</i> $\bar{1}$	<i>P</i> ₂ / <i>n</i>
<i>a</i> /Å	13.0444(7)	12.4292(3)	12.7029(11)	14.2979(5)	12.6840(3)	17.9685(12)
<i>b</i> /Å	25.1790(8)	14.9752(3)	13.9070(9)	14.4497(4)	13.9061(4)	12.0218(9)
<i>c</i> /Å	27.2213(15)	15.4239(4)	14.0718(11)	17.7524(6)	14.0616(3)	20.6526(14)
α /deg	90	116.434(2)	83.944(4)	90	84.128(2)	90
β /deg	90	101.694(3)	78.912(3)	93.934(2)	78.951(3)	93.465(4)
γ /deg	90	100.072(2)	67.302(4)	90	67.239(2)	90
<i>V</i> /Å ³	8940.7(7)	2399.52(12)	2249.2(3)	3659.0(2)	2243.63(10)	4453.1(5)
<i>Z</i>	8	2	2	4	2	4
<i>D</i> _{calc} /g cm ⁻³	1.408	1.298	1.363	1.375	1.222	1.545
μ (Mo K α)/mm ⁻¹	3.671	1.035	3.650	1.461	1.056	4.001
<i>F</i> (000)	3832	986	986	1564	858	2076
reflections collected	56365	75230	17318	24898	64198	29698
independent reflections	8412	9058	7858	6924	8432	8408
observed reflections [<i>I</i> > 2 σ (<i>I</i>)]	5552	8644	5985	5519	7616	5064
<i>R</i> _{int}	0.108	0.052	0.083	0.061	0.061	0.072
parameters refined	478	523	505	416	505	460
<i>R</i> ₁	0.051	0.060	0.060	0.031	0.049	0.061
w <i>R</i> ₂	0.117	0.171	0.152	0.067	0.136	0.147
<i>S</i>	1.019	1.116	1.010	1.014	1.065	0.997
$\Delta\rho_{\text{min}}$ /e Å ⁻³	-0.64	-1.35	-1.46	-0.40	-0.76	-0.75
$\Delta\rho_{\text{max}}$ /e Å ⁻³	2.32	1.93	2.01	0.52	2.47	1.11

Table 2. Selected Distances (Å) and Angles (deg) in the [M(BH₄)₂(THF)₅]⁺ Cations

M	[M(BH ₄) ₂ (THF) ₅][X]								
	Y ⁷ BPh ₄	Sm ⁷ BPh ₄	Sm ²³ Sm(Cp')(BH ₄) ₃	Nd ⁷ BPh ₄	Nd ⁸ B(C ₆ F ₅) ₄	Ce BPh ₄	U BPh ₄	U ⁵ U ₂ (C ₇ H ₇)(BH ₄) ₆	La ²⁴ La(BH ₄) ₄ (THF) ₂
M···B(1)	2.584(3)	2.688(5)	2.622(8)	2.727(3)	2.596(4)	2.678(6)	2.685(9)	2.72(4)	2.729
M···B(2)	2.569(3)	2.728(6)	2.623(8)	2.740(4)	2.641(4)	2.704(7)	2.697(9)	2.71(4)	2.729
⟨M–O⟩	2.427(21)	2.440(18)	2.485(8)	2.459(19)	2.51(3)	2.534(14)	2.544(15)	2.56(2)	2.567(7)
B(1)–M–B(2)	178.41(10)	178.97(16)	176.6(3)	178.56(13)	177.67(13)	176.15(19)	177.6(3)	176(1)	177.2
⟨O–M–O⟩	72(1)	72(3)	72(1)	72(3)	72(2)	72(3)	72(2)	72(1)	72(1)

distilled immediately before use. IR samples were prepared as Nujol mulls between KBr round cell windows, and the spectra were recorded on a Perkin-Elmer FT-IR 1725X spectrometer. The ¹H NMR spectra were recorded on a Bruker DPX 200 instrument and referenced internally using the residual protio solvent resonances relative to tetramethylsilane (δ 0); ¹¹B chemical shifts are relative to BF₃·Et₂O as external reference. The spectra were recorded at 23 °C when not otherwise specified. Elemental analyses were performed by Analytische Laboratorien at Lindlar (Germany). 18-Crown-6 and 18-thiacrown-6 (Fluka) were dried under vacuum before use. [M(BH₄)₃(THF)₃] (M = Nd,^{5b} Ce,¹² U¹³) and [NEt₃H][BPh₄]^{5b} were synthesized as previously reported.

Synthesis of [U(BH₄)₂(THF)₅][BPh₄] (1). A flask was charged with [U(BH₄)₃(THF)₃] (135.9 mg, 0.27 mmol) and [NEt₃H][BPh₄] (114.9 mg, 0.27 mmol) and THF (30 mL) was condensed in it. After stirring for 2 h at 20 °C, the brown solution was filtered and evaporated to dryness, leaving a brown powder of **1** which was contaminated with NEt₃·BH₃, as shown by the ¹H NMR spectra. The latter was eliminated after dissolution of the powder in THF (20 mL) and evaporation of the solution under vacuum; this operation was repeated three times, leading eventually to the analytically pure product **1**. Yield: 237.0 mg (92%). Anal. Calcd for C₄₄H₆₈B₃O₅U: C, 55.75; H, 7.18; B, 3.48. Found: C, 55.61; H, 7.11; B, 3.31. ¹H NMR (THF-*d*₈): δ 9.5 (br s, *w*_{1/2} = 315 Hz, 8 H, BH₄), 7.68 (s, 8 H, Ph), 6.89 (s, 8 H, Ph), 6.63 (s, 4 H, Ph). ¹H

NMR (pyridine-*d*₅): δ 77.4 (br s, *w*_{1/2} = 350 Hz, 8 H, BH₄), 7.72 (s, 8 H, Ph), 7.15 (s, 12 H, Ph), 3.64 and 1.56 (m, 2 × 20 H, THF). ¹¹B{¹H} NMR (pyridine-*d*₅): δ 232.53 (s, BH₄), -5.53 (s, BPh₄). IR (Nujol): ν /cm⁻¹ 2425s (B–H_i stretching), 2218s and 2162s (B–H_b stretching). Brown crystals of **1** suitable for X-ray diffraction were obtained by crystallization from THF.

Synthesis of [Nd(BH₄)₂(THF)₅][BPh₄] (2). Following the same procedure as for **1**, [Nd(BH₄)₃(THF)₃] (296.1 mg, 0.73 mmol) reacted with [NEt₃H][BPh₄] (337.5 mg, 0.80 mmol) to give a pale violet powder of [Nd(BH₄)₂(THF)₅][BPh₄]. Yield: 333.2 mg (71%). Anal. Calcd for C₃₂H₄₄B₃O₂Nd: C, 60.30; H, 6.96; B, 5.09. Found: C, 59.95; H, 6.89; B, 4.85. ¹H NMR (THF-*d*₈): δ 90.1 (br s, *w*_{1/2} = 305 Hz, 8 H, BH₄), 7.32 (s, 8 H, Ph), 6.78 (s, 8 H, Ph), 6.64 (s, 4 H, Ph). ¹H NMR (pyridine-*d*₅): δ 87.2 (br s, *w*_{1/2} = 350 Hz, 8 H, BH₄), 7.73 (m, 20 H, Ph), 3.66 and 1.61 (m, 2 × 4 H, THF). ¹¹B{¹H} NMR (pyridine-*d*₅): δ 157.42 (s, BH₄), -6.60 (s, BPh₄). IR (Nujol): ν /cm⁻¹ 2436s (B–H_i stretching), 2226s and 2168s (B–H_b stretching). Pale violet crystals of **2** suitable for X-ray diffraction were obtained by crystallization from THF.

Synthesis of [Ce(BH₄)₂(THF)₅][BPh₄] (3). Following the same procedure as for **1**, [Ce(BH₄)₃(THF)₃] (284.0 mg, 0.71 mmol) reacted with [NEt₃H][BPh₄] (358.1 mg, 0.85 mmol) to give an off-white powder of [Ce(BH₄)₂(THF)₅][BPh₄]. Yield: 372.1 mg (74%). Anal. Calcd for C₄₀H₆₀B₃O₄Ce: C, 61.80; H, 7.78; B, 4.17. Found: C, 61.89; H, 7.85; B, 4.26. ¹H NMR (THF-*d*₈): δ 29.3 (br s, *w*_{1/2} = 425 Hz, 8 H, BH₄), 7.20 (s, 8 H, Ph), 6.79 (s, 8 H, Ph), 6.65 (s, 4 H, Ph). ¹H NMR (pyridine-*d*₅): δ 32.3 (br s, *w*_{1/2} = 365 Hz, 8 H, BH₄), 8.05 (s, 8 H, Ph), 7.25 (s, 12 H, Ph), 3.67 and 1.64 (m, 2 × 8 H, THF). ¹¹B{¹H} NMR (pyridine-*d*₅): δ 15.34 (s, BH₄), -6.49

(12) Roger, M.; Arliguie, T.; Thuéry, P.; Fourmigué, M.; Ephritikhine, M. *Inorg. Chem.* **2005**, *44*, 584.

(13) (a) Schlessinger, H. I.; Brown, H. C. *J. Am. Chem. Soc.* **1953**, *75*, 219. (b) Baudry, D.; Bulot, E.; Charpin, P.; Ephritikhine, M.; Lance, M.; Nierlich, M.; Vigner, J. *J. Organomet. Chem.* **1989**, *371*, 155.

(s, BPh₄). IR (Nujol): ν/cm^{-1} 2432s (B–H_i stretching), 2219s and 2170s (B–H_b stretching). Colorless crystals of **3**·C₄H₈S suitable for X-ray diffraction were obtained from a solution of **3** and 18-thiacrown-6 in the minimum amount of THF, diluted by tetrahydrothiophene (1:7).

Synthesis of [U(BH₄)₂(18-crown-6)][BPh₄] (4). A flask was charged with **1** (78.0 mg, 0.082 mmol) and 18-crown-6 (22.0 mg, 0.083 mmol) and THF (30 mL) was condensed in it. After stirring for 2 h at 20 °C, the yellow solution deposited yellow crystals of **4**. The solvent was evaporated off, and the product was washed with diethyl ether (10 mL) and dried under vacuum. Yield: 63.5 mg (91%). Anal. Calcd for C₃₆H₅₂B₃O₆U: C, 50.79; H, 6.16; B, 3.81. Found: C, 50.53; H, 6.32; B, 3.70. ¹H NMR (pyridine-*d*₅): δ 71.1 (br s, $w_{1/2}$ = 285 Hz, 8 H, BH₄), 8.03 (s, 8 H, Ph), 7.21 (s, 12 H, Ph), 4.54 (s, 24 H, 18-crown-6). ¹¹B{¹H} NMR (pyridine-*d*₅): δ 275.95 (s, BH₄), –5.85 (s, BPh₄). IR (Nujol): ν/cm^{-1} 2441s (B–H_i stretching), 2206s and 2156s (B–H_b stretching). Crystals of **4**·THF suitable for X-ray diffraction were obtained by slowly cooling a hot solution of **1** (7.2 mg, 7.57 μmol) and 18-crown-6 (3.0 mg, 11.3 μmol) in THF (0.4 mL).

Synthesis of [Nd(BH₄)₂(18-crown-6)][BPh₄] (5). Following the same procedure as for **4**, **2** (85.0 mg, 0.10 mmol) reacted with 18-crown-6 (26.0 mg, 0.10 mmol) to give a pale blue powder of **5**. Yield: 62.2 mg (82%). Anal. Calcd for C₃₆H₅₂B₃O₆Nd: C, 57.19; H, 6.92. Found: C, 57.08; H, 6.93. ¹H NMR (pyridine-*d*₅): δ 125.7 (br s, $w_{1/2}$ = 450 Hz, 8 H, BH₄), 7.82 (s, 8 H, Ph), 7.23 (s, 12 H, Ph), 0.52 (s, 24 H, 18-crown-6). ¹¹B{¹H} NMR (pyridine-*d*₅): δ 201.42 (s, BH₄), –5.67 (s, BPh₄). IR (Nujol): ν/cm^{-1} 2446s (B–H_i stretching), 2210s and 2160s (B–H_b stretching). Crystals of **5** suitable for X-ray diffraction were obtained by crystallization from THF.

Synthesis of [Ce(BH₄)₂(18-crown-6)][BPh₄] (6). Following the same procedure as for **4**, [Ce(BH₄)₂(THF)₄][BPh₄] (174.6 mg, 0.22 mmol) reacted with 18-crown-6 (98.0 mg, 0.37 mmol) to give an off-white powder of **6**. Yield: 121.5 mg (72%). Anal. Calcd for C₃₆H₅₂B₃O₆Ce: C, 57.40; H, 6.96; B, 4.31. Found: C, 57.21; H, 6.86; B, 4.07. ¹H NMR (pyridine-*d*₅): δ 54.2 (br s, $w_{1/2}$ = 425 Hz, 8 H, BH₄), 7.92 (s, 8 H, Ph), 7.25 (s, 12 H, Ph), 0.65 (s, 24 H, 18-crown-6). IR (Nujol): ν/cm^{-1} 2445s (B–H_i stretching), 2210s and 2162s (B–H_b stretching). Crystals of **6**·THF suitable for X-ray diffraction were obtained by crystallization from THF.

Synthesis of [U(BH₄)₂(18-thiacrown-6)][BPh₄] (7). A flask was charged with **1** (63.0 mg, 0.066 mmol) and 18-thiacrown-6 (24.0 mg, 0.066 mmol) in tetrahydrothiophene (30 mL). The reaction mixture was stirred for 2 h, and the red solution deposited a red powder of **7** which, after filtration, was dried under vacuum. Yield: 47.7 mg (76%). Anal. Calcd for C₃₆H₅₂B₃S₆U: C, 45.63; H, 5.53; S, 20.30. Found: C, 45.87; H, 5.71; S, 19.89. The poor solubility of **7** in organic solvents prevented the collection of NMR spectra. IR (Nujol): ν/cm^{-1} 2463s (B–H_i stretching), 2184s and 2116s (B–H_b stretching). Red crystals of **7**·C₄H₈S were picked from the reaction mixture, before filtration and evaporation to dryness.

Crystallographic Data Collection and Structure Determination. The data were collected at 100(2) K on a Nonius Kappa-CCD area detector diffractometer¹⁴ using graphite-monochromated Mo K α radiation (λ = 0.71073 Å). The crystals were introduced into glass capillaries with a protecting “Paratone-N” oil (Hampton Research) coating. The unit cell parameters were determined from ten frames, then refined on all data. The data were processed with HKL2000.¹⁵ The structures were solved by direct methods or by Patterson map interpretation with SHELXS-97, expanded by

subsequent Fourier-difference synthesis and refined by full-matrix least-squares on F^2 with SHELXL-97.¹⁶ Absorption effects were corrected empirically with the program DELABS.¹⁷ All non-hydrogen atoms were refined with anisotropic displacement parameters. The borohydride protons were found on Fourier-difference maps for all compounds, and the carbon-bound hydrogen atoms were introduced at calculated positions. All hydrogen atoms were treated as riding atoms with an isotropic displacement parameter equal to 1.2 times that of the parent atom. In compounds **4** and **6**, the two THF solvent molecules were given 0.5 occupancy factors to retain acceptable displacement parameters and/or to account for their closeness to their image by symmetry, and they were refined with restraints on bond lengths and displacement parameters (a short H···H contact involving a THF proton is likely due to the poor resolution, and resulting imperfect location, of these molecules).

Crystal data and structure refinement parameters are given in Table 1. The molecular plots were drawn with SHELXTL.¹⁶

Computational Details. The calculations were performed using DFT¹⁸ with the ADF2007.01 (Amsterdam Density Functional) code.^{18f} Scalar relativistic effects were introduced within the Zero Order Regular Approximation (ZORA).¹⁹ The DFT/ZORA method has been successfully used to investigate both experimental geometries and electronic structure of heavy f-element compounds with a satisfying accuracy.^{19c–e} Spin–orbit effects were not taken into account. Triple- ζ Slater-type valence orbitals (STO) augmented by one set of polarization functions were used for all atoms. The frozen-core approximation where the core density is obtained from four-component Dirac–Slater calculations has been applied for all atoms. The 1s core electrons were frozen for the boron, carbon, and oxygen atoms during molecular calculations. For heavy elements, the Ce[4d] and U[5d] valence spaces include the 4f/5s/5p/5d/6s/6p and 5f/6s/6p/6d/7s/7p shells (11 and 14 valence electrons) respectively. The Vosko–Wilk–Nusair functional^{20a} for the local density approximation (LDA) and the gradient corrections for exchange and correlation of Becke and Perdew,^{20b–e} respectively, have been used. Complete ZORA/BP86/TZP geometry optimization for the ground states of the highest spin-multiplet state was first carried out and was followed by analytical vibrational frequencies calculations, to check the nature of the stationary point (minimum or transition state). Molecular orbital plots and geometries were generated using the ADFview program.^{18f}

Results and Discussion

Synthesis of the Complexes. The protonolysis reaction of a metal-borohydride bond by means of an acidic ammonium salt represents a convenient access to cationic complexes which was previously used for the preparation

(16) Sheldrick, G. M. *Acta Crystallogr., Sect. A* **2008**, *64*, 112.

(17) Spek, A. L. *J. Appl. Crystallogr.* **2003**, *36*, 7.

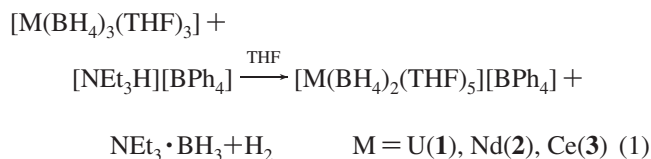
(18) (a) Baerends, E. J.; Ellis, D. E.; Ros, P. *Chem. Phys.* **1973**, *2*, 41. (b) Versluis, L.; Ziegler, T. *J. Chem. Phys.* **1988**, *88*, 322. (c) te Velde, G.; Baerends, E. J. *J. Comput. Phys.* **1992**, *99*, 84. (d) van Lenthe, E.; Snijders, J. G.; Baerends, E. J. *J. Chem. Phys.* **1996**, *105*, 6505. (e) te Velde, G.; Bickelhaupt, F. M.; Baerends, E. J.; Fonseca, G. C.; van Gisbergen, S. J. A.; Snijders, J. G.; Ziegler, T. *J. Comput. Chem.* **2001**, *22*, 931. (f) *ADF2007.01, SCM*; Theoretical Chemistry, Vrije University: Amsterdam, The Netherlands; <http://www.scm.com>.

(19) (a) Fonseca, G. C.; Snijders, J. G.; te Velde, G.; Baerends, E. J. *Theor. Chem. Acc.* **1998**, *391*. (b) van Lenthe, E.; Ehlers, A.; Baerends, E. J. *J. Chem. Phys.* **1999**, *110*, 8943. (c) Shamov, G. A.; Schreckenbach, G. *J. Phys. Chem. A* **2005**, *109*, 10961. (d) BenYahia, M.; Belkhir, L.; Boucekkine, A. *J. Mol. Struct. (Theo. Chem.)* **2006**, *777*, 61. (e) Gaunt, A. J.; Reilly, S. D.; Enriquez, A. E.; Scott, B. J.; Ibers, J. A.; Sekar, P.; Ingram, K. I. M.; Kaltsoyannis, N.; Neu, M. P. *Inorg. Chem.* **2008**, *47*, 29. (f) Ingram, K. I. M.; Tassell, M. J.; Gaunt, A. J.; Kaltsoyannis, N. *Inorg. Chem.* **2008**, *47*, 78524.

(14) Hooft, R. W. W. *COLLECT*; Nonius BV: Delft, The Netherlands, 1998.

(15) Otwinowski, Z.; Minor, W. *Methods Enzymol.* **1997**, *276*, 307.

of $[\text{Nd}(\text{COT})(\text{THF})_4][\text{BPh}_4]$ ($\text{COT} = \text{C}_8\text{H}_8$), a first example of a cyclooctatetraenyl lanthanide cation,⁵ and of $[\text{U}(\text{COT})\text{-(BH}_4)(\text{THF})_2][\text{BPh}_4]$ and $[\text{U}(\text{COT})(\text{L})_3][\text{BPh}_4]_2$ [$\text{L} = \text{OPPh}_3$, $\text{OP}(\text{NMe}_2)_3$], which are, respectively, the first cationic organometallic borohydride and the first organometallic dication of an f element.²¹ The cationic complexes $[\text{M}(\text{BH}_4)_2(\text{THF})_5][\text{BPh}_4]$ [$\text{M} = \text{U}$ (**1**), Nd (**2**), and Ce (**3**)] were readily synthesized by reaction of the neutral precursors $[\text{M}(\text{BH}_4)_3(\text{THF})_3]$ and $[\text{NEt}_3\text{H}][\text{BPh}_4]$ in THF, according to eq 1. By following a similar procedure, Okuda et al. have independently isolated **2** and the other derivatives with $\text{Ln} = \text{Y}$, Sm , and La .⁷ After elimination of the $\text{NEt}_3\cdot\text{BH}_3$ byproduct by washing with THF or successive evaporations of THF solutions, and drying under vacuum, powders of **1** (brown), $[\text{Nd}(\text{BH}_4)_2(\text{THF})_2][\text{BPh}_4]$ (pale violet), and $[\text{Ce}(\text{BH}_4)_2(\text{THF})_4][\text{BPh}_4]$ (white) were isolated with yields of 92, 71, and 74%, respectively; these powders were characterized by their elemental analyses (C, H, B) and their ¹H NMR spectra in THF and pyridine which exhibit, in addition to the resonances of the $[\text{BPh}_4]^-$ anion, a broad high field signal attributed to the equivalent BH_4 ligands and the peaks corresponding to the free THF molecules which were displaced from the metal by the solvent. It is likely that the dissociation of the THF ligands from **2** and **3** under vacuum, which was apparently not observed by Okuda et al.,⁷ is related to the formation of zwitterionic complexes with phenyl groups of BPh_4 coordinated to the metal atom. Such π coordination of tetraphenylborate and related anions to metal centers is well documented and was observed, for example, with the powder of $[\text{U}(\text{NEt}_2)_3(\eta\text{-Ph})_2\text{BPh}_2]$ which was isolated after drying the crystals of $[\text{U}(\text{NEt}_2)_3(\text{THF})_3][\text{BPh}_4]$ under vacuum.²²



Crystals of **1** were obtained by crystallization from THF while crystals of **3**· $\text{C}_4\text{H}_8\text{S}$ were deposited from a solution of **3** and 18-thiacrown-6 in a mixture of THF and tetrahydrothiophene, in an attempt at the synthesis of $[\text{Ce}(\text{BH}_4)_2(18\text{-thiacrown-6})][\text{BPh}_4]$ (vide infra). The $[\text{U}(\text{BH}_4)_2(\text{THF})_5]^+$ cation was previously encountered in the crystals of the inverse cycloheptatrienyl sandwich complex $[\text{U}(\text{BH}_4)_2(\text{THF})_5][(\text{BH}_4)_3\text{U}(\mu\text{-C}_7\text{H}_7)\text{U}(\text{BH}_4)_3]$ which were obtained fortuitously during purification of $\text{K}[(\text{BH}_4)_3\text{U}(\mu\text{-C}_7\text{H}_7)\text{U}(\text{BH}_4)_3]$.⁶ In addition to the aforementioned crystals of $[\text{Ln}(\text{BH}_4)_2(\text{THF})_5][\text{BPh}_4]$ ($\text{Ln} = \text{Y}$, Sm , Nd),⁷ and $[\text{Nd}(\text{BH}_4)_2(\text{THF})_5][\text{B}(\text{C}_6\text{F}_5)_4]$,⁸ the lanthanide cations $[\text{Ln}(\text{BH}_4)_2(\text{THF})_5]^+$ ($\text{Ln} = \text{Sm}$, La) were found in the crystals

of $[\text{Sm}(\text{BH}_4)_2(\text{THF})_5][\text{Sm}(\text{C}_5\text{Me}_4\text{Pr})(\text{BH}_4)_3]^{23}$ and $[\text{La}(\text{BH}_4)_2(\text{THF})_5][\text{La}(\text{BH}_4)_4(\text{THF})_2]$,²⁴ which were formed, respectively, by partial hydrolysis of $[\text{Sm}(\text{C}_5\text{Me}_4\text{Pr})(\text{BH}_4)_2(\text{THF})]$ in toluene and crystallization of $[\text{La}(\text{BH}_4)_3(\text{THF})_3]$ from THF.

Treatment of complexes **1–3** with 18-crown-6 in THF led to the immediate formation of the crown ether derivatives $[\text{M}(\text{BH}_4)_2(18\text{-crown-6})][\text{BPh}_4]$ [$\text{M} = \text{U}$ (**4**), Nd (**5**), Ce (**6**)] which, after evaporation of the solvent and washing with diethyl ether, were isolated as a yellow (U), pale blue (Nd), or white (Ce) powder in 91, 82, and 72% yield, respectively. Crystals of **4**·THF, **5**, and **6**·THF were deposited from THF solutions. The $[\text{U}(\text{BH}_4)_2]^+$ cation was previously found inserted into the dicyclohexyl-(18-crown-6) ether (dcc) in the complex $[\text{U}(\text{BH}_4)_2(\text{dcc})][\text{UCl}_5(\text{BH}_4)]$ which was obtained accidentally after partial oxidation of $[\text{U}_3(\text{BH}_4)_9(\text{dcc})_2]$ in dichloromethane.²⁵

The IR spectrum of **1**, which exhibits the characteristic absorptions of tridentate BH_4 ligands, that is, a strong sharp band at 2425 cm^{-1} and two strong bands at 2218 and 2162 cm^{-1} assigned, respectively, to the terminal hydrogen–boron stretch $\nu(\text{B-H}_t)$ and bridging hydrogen–boron stretch $\nu(\text{B-H}_b)$, is essentially identical with those of the neodymium and cerium counterparts **2** and **3**; these spectra are also very similar to those of the 18-crown-6 derivatives **4–6**. Identical borohydride band patterns were observed in the IR spectra of various pairs of analogous complexes like $\text{M}(\text{BH}_4)_4$ ($\text{M} = \text{Zr}$, Hf),²⁶ $[\text{M}(\text{C}_5\text{H}_5)_2(\text{BH}_4)_2]$ ($\text{M} = \text{Zr}$, Hf),²⁷ or $[\text{M}(\text{C}_5\text{H}_5)_2(\text{BH}_4)]$ ($\text{M} = \text{V}$, Nb),²⁸ in line with the very similar geometries and bonding of these compounds; this trend also indicates that the mass of the metal has insignificant effect upon the structurally diagnostic vibrations. However, the IR spectra of $[\text{M}(\text{C}_5\text{H}_5)_2(\text{BH}_4)]$ ($\text{M} = \text{V}$, Nb) show, in comparison to that of $\text{M} = \text{Ti}$, a marked lowering of $\nu(\text{B-H}_b)$ while the vibrations involving the $\text{B}(\text{H}_t)_2$ portion of the complex remain unperturbed. This striking anomaly was explained by the effects of increasing metal ion distortion of the isolated BH_4^- unit and decreasing the ionic character of the bonding.²⁸

The THF ligands of **1** were not displaced with the hexathia macrocycle 18-thiacrown-6 in THF but, in tetrahydrothiophene, **1** was readily transformed into $[\text{U}(\text{BH}_4)_2(18\text{-thiacrown-6})][\text{BPh}_4]$ (**7**) which crystallized as the red solvate **7**· $\text{C}_4\text{H}_8\text{S}$. Complex **7** is, after the iodide compounds $[\text{Ml}_3(9\text{-thiacrown-3})(\text{MeCN})_2]$ ($\text{M} = \text{U}$, La),^{10e} a novel example of a crown thioether complex of an f element. Attempts at the synthesis of the lanthanide analogues of **7** were unsuccessful; in contrast to **1**, complexes **2** and **3** are poorly soluble in tetrahydrothiophene, and their THF ligands could not be

- (20) (a) Vosko, S. D.; Wilk, L.; Nusair, M. *Can. J. Chem.* **1990**, *58*, 1200. (b) Becke, A. D. *J. Chem. Phys.* **1986**, *84*, 4524. (c) Becke, A. D. *Phys. Rev. A* **1988**, *38*, 3098. (d) Perdew, J. P. *Phys. Rev. B* **1986**, *33*, 8822. (e) Perdew, J. P. *Phys. Rev. B* **1986**, *34*, 7406.
- (21) Cendrowski-Guillaume, S. M.; Lance, M.; Nierlich, M.; Ephritikhine, M. *Organometallics* **2000**, *19*, 3257.
- (22) Berthet, J. C.; Boisson, C.; Lance, M.; Vigner, J.; Nierlich, M.; Ephritikhine, M. *J. Chem. Soc., Dalton Trans.* **1995**, 3019.

- (23) Bonnet, F.; Visseaux, M.; Hafid, A.; Baudry-Barbier, D.; Kubicki, M. M.; Vigier, E. *Inorg. Chem. Commun.* **2007**, *10*, 690.
- (24) Bel'skii, V. K.; Sobolev, A. N.; Bulychev, B. M.; Alikhanova, T. K.; Kurbonbekov, A.; Mirsaidov, U. *Koord. Khim.* **1990**, *16*, 1693.
- (25) Dejean, A.; Charpin, P.; Folcher, G.; Rigny, P.; Navaza, A.; Tsoucaris, G. *Polyhedron* **1987**, *6*, 189.
- (26) Marks, T. J.; Kennelly, W. J.; Kolb, J. R.; Shimp, L. *Inorg. Chem.* **1972**, *11*, 2540.
- (27) Johnson, P. L.; Cohen, S. A.; Marks, T. J.; Williams, J. M. *J. Am. Chem. Soc.* **1978**, *100*, 2709.
- (28) Marks, T. J.; Kennelly, W. J. *J. Am. Chem. Soc.* **1975**, *97*, 1439.

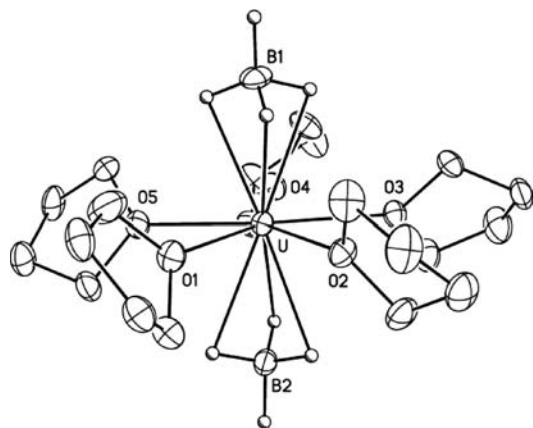


Figure 1. View of the cation of $[\text{U}(\text{BH}_4)_2(\text{THF})_5][\text{BPh}_4]$ (**1**). The hydrogen atoms have been omitted, except those of the borohydride ligands. The displacement ellipsoids are drawn at the 30% probability level.

exchanged with sulfur-containing molecules. This difference could reflect the softer (less hard) character of the 5f versus 4f trivalent ion, leading to a better affinity of soft ligands for the actinide. It is during these attempts that crystals of $3 \cdot \text{C}_4\text{H}_8\text{S}$ were obtained.

Crystal Structures. The $[\text{M}(\text{BH}_4)_2(\text{THF})_5]^+$ cations of complexes **1** and **3** adopt a pentagonal bipyramidal configuration with the oxygen atoms of the THF ligands in the equatorial plane and the borohydride ligands in apical positions. This structure is also that adopted by a series of $[\text{LnX}_2(\text{THF})_5]^+$ cations ($\text{X} = \text{Cl}$ or I).²⁹ A view of the uranium complex **1** is shown in Figure 1; selected bond lengths and angles in the cations of **1** and $3 \cdot \text{C}_4\text{H}_8\text{S}$ are listed in Table 2, together with those of the previously reported $[\text{M}(\text{BH}_4)_2(\text{THF})_5]^+$ cations ($\text{M} = \text{Y},^7 \text{Sm},^{7,23} \text{Nd},^{7,8} \text{La},^{24} \text{U}^5$) for comparison. The $\text{M}-\text{O}$ distances are unexceptional, and the short $\text{M} \cdots \text{B}$ distances indicate a tridentate ligation mode of the BH_4 ligands, in keeping with the positions found for the hydrogen atoms.

Variations in the strength of $\text{M}-\text{X}$ bonds in analogous uranium(III) and lanthanide(III) complexes ($\text{X} = \text{C}, \text{N}, \text{P}, \text{I}, \text{S}$), showing the more covalent character of the $\text{U}-\text{X}$ bond, have previously been detected through the deviations Δ corresponding to the differences $\{\langle \text{U}-\text{X} \rangle - \langle \text{Ln}-\text{X} \rangle\}$ and $\{r(\text{U}^{3+}) - r(\text{Ln}^{3+})\}$, $r(\text{M}^{3+})$ being the ionic radius of the metal.³⁰ These deviations are generally small and hardly significant (0.02–0.05 Å), but they are as high as 0.1 Å in

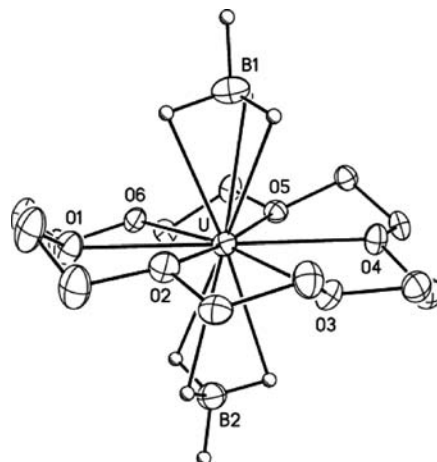


Figure 2. View of the cation of $[\text{U}(\text{BH}_4)_2(18\text{-crown-6})][\text{BPh}_4]$ (**4**). The hydrogen atoms have been omitted, except those of the borohydride ligands. The displacement ellipsoids are drawn at the 30% probability level.

the phosphorus complexes $[\text{M}(\text{C}_5\text{H}_4\text{Me})_3(\text{L})]$ [$\text{M} = \text{Ce}$ or U ; $\text{L} = \text{PMe}_3$ or $\text{P}(\text{OCH}_2)_3\text{CEt}$]^{10a} and in the tris(btp) compounds $[\text{M}(\text{btp})_3]\text{I}_3$ ($\text{M} = \text{La}, \text{Ce}, \text{Sm}$, or U ; $\text{btp} = 2,6$ -dialkyl-1,2,4-triazin-3-yl)pyridine),^{9d} and $\Delta = 0.2$ Å in the terpyridine compounds $[\text{M}(\text{C}_5\text{Me}_5)_2(\text{terpy})]\text{I}$ ($\text{M} = \text{Ce}, \text{U}$).^{9k} These greatest deviations were explained by the softer character and better π -accepting ability of the phosphorus- and nitrogen-containing ligands. However, examining the bond length variations in the present series appears inconclusive when the $\pm 3\sigma$ confidence interval is taken into account. Okuda et al. already noted that the $\text{Sm} \cdots \text{B}$ distances in $[\text{Sm}(\text{BH}_4)_2(\text{THF})_5][\text{BPh}_4]$ ⁷ differ from those measured in the cation of $[\text{Sm}(\text{BH}_4)_2(\text{THF})_5][\text{Sm}(\text{C}_5\text{Me}_4\text{Pr})(\text{BH}_4)_3]$,²³ the difference is even larger between the $\text{Nd} \cdots \text{B}$ distances of $[\text{Nd}(\text{BH}_4)_2(\text{THF})_5][\text{X}]$ with $\text{X} = \text{BPh}_4$ ⁷ or $\text{B}(\text{C}_6\text{F}_5)_4$.⁸ It can also be seen that the difference of -0.03 Å between the $\text{Nd} \cdots \text{B}$ and $\text{Ce} \cdots \text{B}$ distances of $[\text{Ln}(\text{BH}_4)_2(\text{THF})_5][\text{BPh}_4]$ ($\text{Ln} = \text{Nd}, \text{Ce}$) is not of the expected sign. These discrepancies can be explained by the compounds being not isostructural, the counteranions being not identical, and the crystal data having been collected under different experimental conditions.

Contrary to the structures of the $[\text{M}(\text{BH}_4)_2(\text{THF})_5]^+$ cations, those of the $[\text{M}(\text{BH}_4)_2(18\text{-crown-6})]^+$ cations ($\text{M} = \text{U}, \text{Nd}, \text{Ce}$), and especially the uranium and cerium derivatives **4**·THF and **6**·THF, which are isomorphous, would permit a rigorous comparison of their geometrical parameters. A view of the cation of **4** is shown in Figure 2 and selected bond lengths and angles in complexes **4–6** are listed in Table 3. The metal center is in a slightly distorted hexagonal bipyramidal environment, with the six oxygen atoms of the crown ether in the equatorial plane and the BH_4 groups at the apexes. Such $[\text{LnX}_2(18\text{-crown-6})]^+$ cations are, to the best of our knowledge, limited to $\text{X} = \text{NO}_3$ in $[\text{Ln}(\text{NO}_3)_2(18\text{-crown-6})_3][\text{Ln}(\text{NO}_3)_6]$ ($\text{Ln} = \text{Nd},^{31a} \text{Gd}^{31b}$); the chloride analogues have an additional ligand in their coordination sphere, like $[\text{LnCl}_2(18\text{-crown-6})(\text{H}_2\text{O})]\text{Cl}$.^{31c} The structures of the cations of **4–6** are quite similar to those of the neutral complexes $[\text{M}(\text{BH}_4)_2(18\text{-crown-6})]$ ($\text{M} = \text{Sr}, \text{Ba}$) in which the crown features crystallographically imposed D_{3d} sym-

- (29) (a) Willey, G. R.; Woodman, T. J.; Carpenter, D. J.; Errington, W. *J. Chem. Soc., Dalton Trans.* **1997**, 2677. (b) Willey, G. R.; Aris, D. R.; Errington, W. *Inorg. Chim. Acta* **2001**, 318, 97. (c) Evans, W. J.; Shreeve, J. L.; Ziller, J. W.; Doedens, R. *J. Inorg. Chem.* **1995**, 34, 576. (d) Willey, G. R.; Meehan, P. R.; Woodman, T. J.; Drew, M. G. B. *Polyhedron* **1997**, 16, 623. (e) Deacon, G. B.; Feng, T.; Junk, P. C.; Skelton, B. W.; Sobolev, A. N.; White, A. H. *Aust. J. Chem.* **1998**, 51, 75. (f) Roesky, P. W. *Organometallics* **2002**, 21, 4756. (g) Anfang, S.; Karl, M.; Faza, N.; Massa, W.; Magull, J.; Dehnicke, K. *Z. Anorg. Allg. Chem.* **1997**, 623, 1425. (h) Huebner, L.; Kornienko, A.; Emge, T. J.; Brennan, J. G. *Inorg. Chem.* **2004**, 43, 5659. (i) Xie, Z.; Chiu, K. Y.; Wu, B.; Mak, T. C. W. *Inorg. Chem.* **1996**, 35, 5957. (j) Izod, K.; Liddle, S. T.; Clegg, W. *Inorg. Chem.* **2004**, 43, 214.
- (30) Shannon, R. D. *Acta Crystallogr., Sect. A* **1976**, 32, 751.
- (31) (a) Bünzli, J. C. G.; Klein, B.; Wessner, D.; Schenk, K. J.; Chapuis, G.; Bombieri, G.; De Paoli, G. *Inorg. Chim. Acta* **1981**, 54, L43. (b) Nicolo, F.; Bünzli, J. C. G.; Chapuis, G. *Acta Crystallogr. Sect. C* **1988**, 44, 1733. (c) Rogers, R. D.; Rollins, A. N.; Etzenhouser, R. D.; Voss, E. J.; Bauer, C. B. *Inorg. Chem.* **1993**, 32, 3451.

Table 3. Selected Distances (Å) and Angles (deg) in the $[M(BH_4)_2(18\text{-crown-6})]^+$ Cations

M	$[M(BH_4)_2(18\text{-crown-6})][BPh_4]$		
	Nd	Ce	U
$M \cdots B(1)$	2.652(3)	2.684(7)	2.650(12)
$M \cdots B(2)$	2.608(3)	2.692(7)	2.698(12)
$\langle M-O \rangle$	2.640(17)	2.643(14)	2.653(9)
$\langle M-H_b \rangle$	2.43(4)	2.46(5)	2.57(4)
$\langle B-H_b \rangle$	0.9(1)	1.15(8)	1.10(5)
$\langle B-H_i \rangle$	1.0(1)	1.09(5)	1.19(2)
$B(1)-M-B(2)$	174.27(10)	175.5(2)	175.7(4)
$\langle O-M-O \rangle$	60.1(4)	60.2(4)	60.2(6)
$\langle H_b-M-H_b \rangle$	36(4)	43(3)	41.5(9)
$\langle H_b-B-H_b \rangle$	105(7)	104(9)	111(3)
$\langle H_b-B-H_i \rangle$	113(5)	114(3)	107(2)
$\langle M-H_b-B \rangle$	92(7)	88(2)	83(2)

metry.³² The average $M-O$ distances in **4** and **6** are 0.109(7) Å larger than those in **1** and **3**, respectively, reflecting the larger steric hindrance in the former compounds, while the $M \cdots B$ distances are quite identical, showing that the greater number of equatorial donor atoms has no effect on the apical positions. In this case also, the values of the estimated standard deviations do not permit to draw any conclusion about the possible small variations of the $M-O$ and $M \cdots B$ bond lengths; the differences of +0.01 Å between the $U-O$ and the $Ce-O$ distances and of -0.02 Å between the $U \cdots B$ and the $Ce \cdots B$ distances are less than 3 times the standard deviation of the individual distances.

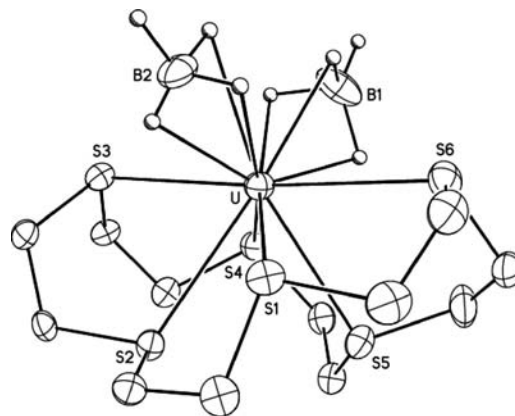
The relationship of the $M \cdots B$ distance to metal ion size for a number of borohydride complexes was already considered to discuss what factors govern these distances as the metal ion and tetrahydroborate ligation geometry are changed.³³ For each series of compounds with bidentate and tridentate BH_4 ligands, the overall correlation between $M \cdots B$ distances and ionic radii was found amazingly linear, considering the large range of metals with distinct oxidation states and coordination numbers, the variety of supporting ligands, and the different methods, temperatures, and phases for which crystal structures were determined. It was therefore pointed out that for most complexes, the variations in $M \cdots B$ distances correspond to those expected from the ionic bonding model, and no conclusion about covalent bonding between the metal atom and the borohydride group could be drawn solely from structural considerations based on the $M \cdots B$ distance. However, disparities were noted within the bidentate structures, with $M \cdots B$ distances varying more than might be expected for comparable ionic radii. In particular, the $Nb \cdots B$ distance in $[Nb(C_5H_5)_2(BH_4)]^{34}$ is 0.11 Å shorter than the $Ti \cdots B$ distance in the isostructural titanium counterpart,³⁵ while the ionic radius of Nb^{3+} is 0.05 Å larger than that of Ti^{3+} .³⁰ This discrepancy was tentatively explained by the more covalent character of the $Nb-BH_4$ bond, in line with the greater volatility of the niobium complex and the unusual features in its IR spectrum (vide supra).

(32) Bremer, M.; Nöth, H.; Thomann, M.; Schmidt, M. *Chem. Ber.* **1995**, *128*, 455.

(33) Edelstein, N. *Inorg. Chem.* **1981**, *20*, 297.

(34) Kirilova, N. I.; Gusev, A. I.; Struchkov, Y. T. *J. Struct. Chem.* **1974**, *15*, 622.

(35) Melmed, K. M.; Coucouvanis, D.; Lippard, S. J. *Inorg. Chem.* **1973**, *12*, 232.

**Figure 3.** View of the cation of $[U(BH_4)_2(18\text{-thiacrown-6})][BPh_4]$ (**7**). The hydrogen atoms have been omitted, except those of the borohydride ligands. The displacement ellipsoids are drawn at the 30% probability level.**Table 4.** Selected Distances (Å) and Angles (deg) in the $[U(BH_4)_2(18\text{-thiacrown-6})]^+$ Cation

$U \cdots B(1)$	2.616(14)	$B(1)-U-B(2)$	99.1(5)
$U \cdots B(2)$	2.605(13)	$S(1)-U-S(2)$	65.11(7)
$U-S(1)$	3.084(3)	$S(2)-U-S(3)$	66.00(7)
$U-S(2)$	3.059(3)	$S(3)-U-S(4)$	63.05(7)
$U-S(3)$	3.064(3)	$S(4)-U-S(5)$	68.75(7)
$U-S(4)$	3.050(3)	$S(5)-U-S(6)$	64.69(8)
$U-S(5)$	3.013(3)	$S(1)-U-S(6)$	66.56(8)
$U-S(6)$	3.101(3)		

Deviation of the geometrical parameters of the coordinated BH_4 ligand from the tetrahedral symmetry of the free BH_4^- anion might give information on the degree of covalency of the metal-ligand bonding. Unfortunately, the position of the hydrogen atoms in the presence of heavy atoms cannot be measured with a good accuracy by X-ray diffraction, and any variation should be regarded with caution and criticism. Considering again the pair of $[M(C_5H_5)_2(BH_4)]$ complexes ($M = Ti, Nb$),^{34,35} it was noted that while the $Nb \cdots B$ distance is smaller than the $Ti \cdots B$ distance, the $Nb-H_b$ bond length is larger than the $Ti-H_b$ bond length, and the H_b-B-H_b angles are larger in the niobium compound. In the present case, the nature of the metal-borohydride bonding in complexes **4** and **6**, being beyond the reach of our experimental approach, was analyzed by relativistic DFT (vide infra).

A view of the $[U(BH_4)_2(18\text{-thiacrown-6})]^+$ cation of **7** is presented in Figure 3, and selected bond lengths and angles are listed in Table 4. The average $U \cdots B$ distance of 2.611(6) Å of the tridentate borohydride ligands, which are in relative *cis* positions, is about 0.07 Å smaller than that of the *trans* diaxial BH_4 groups in the bipyramidal complexes **1** and **4**.

(36) (a) Hartman, J. R.; Wolf, R. E.; Foxman, B. M.; Cooper, S. R. *J. Am. Chem. Soc.* **1983**, *105*, 131. (b) Wolf, R. E.; Hartman, J. R.; Storey, J. M. E.; Foxman, B. M.; Cooper, S. R. *J. Am. Chem. Soc.* **1987**, *109*, 4328.

(37) Junk, P. C.; Atwood, J. L. *Supramol. Chem.* **1994**, *3*, 241.

(38) Fyles, T. M.; Gandour, R. D. *J. Inclusion Phenom.* **1992**, *12*, 313.

(39) (a) Hartman, J. R.; Cooper, S. R. *J. Am. Chem. Soc.* **1986**, *108*, 1202. (b) Helm, M. L.; Helton, G. P.; VanDerveer, D. G.; Grant, G. J. *Inorg. Chem.* **2005**, *44*, 5696. (c) Shaw, J. L.; Wolowska, J.; Collison, D.; Howard, J. A. K.; McInnes, E. J. L.; McMaster, J.; Blake, A. J.; Wilson, C.; Schröder, M. *J. Am. Chem. Soc.* **2006**, *128*, 13827.

(40) Willey, G. R.; Lakin, M. T.; Alcock, N. W. *J. Chem. Soc., Dalton Trans.* **1992**, 1339.

(41) Reed, A. E.; Curtiss, L. A.; Weinhold, F. *Chem. Rev.* **1988**, *88*, 899.

Table 5. Mean Calculated and Experimental (in Square Brackets) Bond Lengths (Å) and Angles (deg) in the $[M(\text{BH}_4)_2(18\text{-crown-6})]^+$ Cations

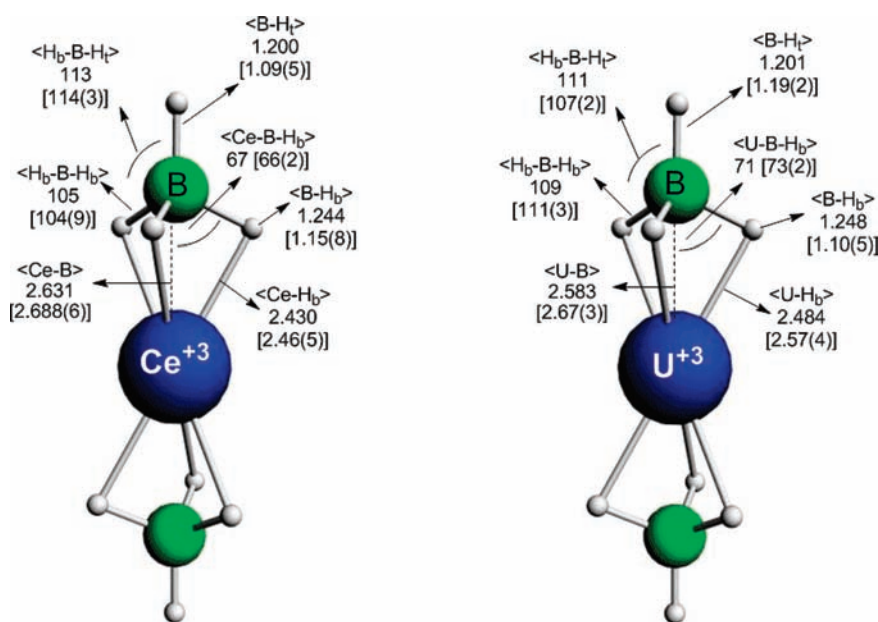
M, spin state	M–O	M–B	M–H _b	B–H _t	B–H _b	M–B–H _b	H _b –B–H _t	H _b –B–H _b
Ce, doublet	2.727 [2.643(14)]	2.631 [2.688(6)]	2.430 [2.46(5)]	1.200 [1.09(5)]	1.244 [1.15(8)]	67 [66(2)]	113 [114(3)]	105 [104(9)]
U, quartet	2.734 [2.653(9)]	2.583 [2.67(3)]	2.484 [2.57(4)]	1.201 [1.19(2)]	1.248 [1.10(5)]	71 [73(2)]	111 [107(2)]	109 [111(3)]

The U–S bond lengths vary from 3.013(3) to 3.101(3) Å and average 3.06(3) Å, a value which is identical to that of 3.05(3) Å measured in $[\text{UI}_3(9\text{-thiacrown-3})(\text{MeCN})_2]^{10e}$. The 18-thiacrown-6 ligand adopts a conformation which can be characterized by the torsion angle sequence for the six groups of S–C, C–C, and C–S bonds, which is (a g⁺ a, ac⁺ g⁺ g⁺, ac[−] g[−] a, g[−] g[−] g[−], a g[−] ac⁺, g[−] g[−] a) where a is *anti* (± 150 to 180°), g *gauche* (30 to 90° or -30 to -90°) and ac *anticlinal* (90 to 150° or -90 to -150°). The S–C–C–S angles are all close to the ideal *gauche* value (in the range 51.3 – 66.0°), whereas the C–S–C–C angles span a wide range, from *gauche* to *anti*, with intermediate *anticlinal*, values. In contrast with crown ethers, thiocrowns show a marked tendency to adopt conformations giving the maximum number of *gauche* arrangements around C–S bonds (as a result of the larger length of C–S versus C–O bonds) and this often results in exodentate positioning of the sulfur atoms; conversely, *anti* arrangements around C–C bonds are favored in thioethers.³⁶ However, this rule suffers some exceptions in free 18-thiacrown-6,^{36,37} with, for example, the sequence (g⁺ a g[−], ac⁺ g⁺ ac[−], ac⁺ a g⁺)₂ for one of the forms known,³⁶ and uranium complexation appears to result in a reversing of these trends in **7** [for comparison, the torsion angles sequence for 18-crown-6 in complexes **4**–**6** is (a g⁺ a, a g[−] a)₃, which corresponds to the very common D_{3d} geometry.³⁸ The conformation adopted in complex **7** results in the molecule having roughly a saddle shape, with the diametrically opposite atoms S3 and S6 bound to uranium in *trans* positions [S3–U–S6 $174.52(8)^\circ$]. The metal atom is thus held on this S3–S6 axis above the basket formed by

the four other sulfur atoms. This is at variance with the central position occupied by the metal in a series of octahedral complexes of general formula $[\text{M}(18\text{-thiacrown-6})]^{n+}$.³⁹ More similitude is found in the complex $[\text{BiCl}_3(18\text{-thiacrown-6})]$, in which the metal ion is located between the thiocrown and the three chlorine atoms, and is nearly coplanar with three sulfur atoms.⁴⁰

Molecular Geometry Optimizations. The molecular structures of the $[\text{M}(\text{BH}_4)_2(18\text{-crown-6})]^+$ cations (M = Ce and U) have been fully optimized at the ZORA/BP86/TZP level (see Computational Details). The highest spin multiplicity has been considered for the U(III) complex bearing the f³ configuration, that is, the quartet state. The spin state of the Ce(III) species is obviously a doublet (f¹ configuration of the metal). Such high spin states are well described by the single determinant configuration Kohn and Sham approach.¹⁸

The most relevant calculated bond distances and angles are reported in Table 5 together with experimental data, for comparison; the optimized molecular geometries are displayed in Figure 4. These calculations give U⋯B distances smaller than Ce⋯B, and U–O bond lengths larger than Ce–O. When the BH₄ coordination geometry is considered, only two deviations in bond lengths are larger than 0.09 Å, that is, 0.11 Å for the B–H_t distance in the cerium complex and 0.15 Å for the B–H_b distance in the uranium counterpart; the deviations in bond angles vary from 0.6 to 2.0°, except that concerning the H_b–B–H_t angle in the U(III) complex, which amounts to 4.3°. Although the U⋯B distance is smaller than the Ce⋯B distance, the U–H_b bond is longer

**Figure 4.** DFT geometries, calculated and experimental (in brackets) bond distances (Å) and angles (deg) of the $[\text{M}(\text{BH}_4)_2(18\text{-crown-6})]^+$ cations (M = Ce, U). The crown-ethers have been omitted for clarity.

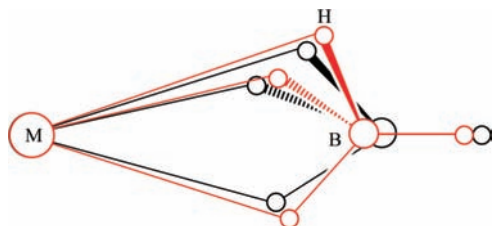


Figure 5. Modifications in the BH_4^- coordination geometry when passing from the cerium (black) to the uranium (red) complexes, from DFT analysis.

than the $\text{Ce}-\text{H}_b$ bond (2.484 versus 2.430 Å), in relation with the opening of the $\text{U}-\text{B}-\text{H}_b$ with respect to the $\text{Ce}-\text{B}-\text{H}_b$ angle (70.7 versus 66.9°), and the larger $\text{H}_b-\text{B}-\text{H}_b$ and smaller $\text{H}_b-\text{B}-\text{H}_t$ angles in the uranium compound. These variations in the geometrical parameters are represented in Figure 5, and they will be discussed further in the light of the electronic structure analysis.

Electronic Structure Calculations. The results of Mulliken Population Analysis (MPA) and Natural Bond Orbital (NBO) analysis are given in Table 6. Although MPA can provide correct global trends, NBO is much more reliable.⁴¹ MPA spin-unrestricted analysis provides metallic spin densities ρ_M and atomic net charges; the value of ρ_M is the difference between the total α and β electronic populations of the metal. Table 6 also contains the MPA $\alpha+\beta$ spin-unrestricted overlap populations relative to the metal–ligand bonding.

The MPA spin density borne by cerium and uranium, 1.03 and 3.11 respectively, correspond to the doublet f^1 and quartet

f^3 states of these atoms in the complexes, implying that no metal-to-ligand back-donation exists at this level. As expected, the Mulliken metallic net charges M^q for both the cerium(III) and uranium(III) borohydride complexes are much smaller than their formal +3 oxidation state. These electronic features reflect a significant ligand-to-metal donation. As given by NBO, this trend is more pronounced for the uranium(III) complex whose metallic net charge, +2.01, is appreciably smaller than that of the cerium(III) analogue, +2.42. It must be pointed out that the charges of the oxygen atoms of the 18-crown-6 ligand are the same in the two complexes, with a value of -0.62 (NBO). However, the $\text{BH}_4^- \rightarrow \text{U(III)}$ donation through the bridging H_b hydrogen atoms is greater in the uranium compound, as shown by the smaller NPA global negative charge of a BH_4^- moiety, that is, -0.65 versus -0.88 in the Ce(III) analogue. The difference between the total charges of the metals is likely due to these distinct $\text{BH}_4^- \rightarrow \text{M(III)}$ donations. MPA leads to the same conclusions. Furthermore, the sum of the three MPA overlap populations of the $\text{M}-\text{H}_b$ bonds is significantly greater in the uranium(III) complex, 0.107 versus 0.073 for Ce(III), and presents a good correlation with the opening of the $\text{H}_b-\text{B}-\text{H}_b$ angle, thus showing a better directional interaction between uranium 5f orbitals and the bridging hydrogen atoms. These results highlight the significant Ce(III)/U(III) differentiation by the borohydride ligand and sustain the hypothesis of stronger covalent interactions between this ligand and the uranium(III) center.

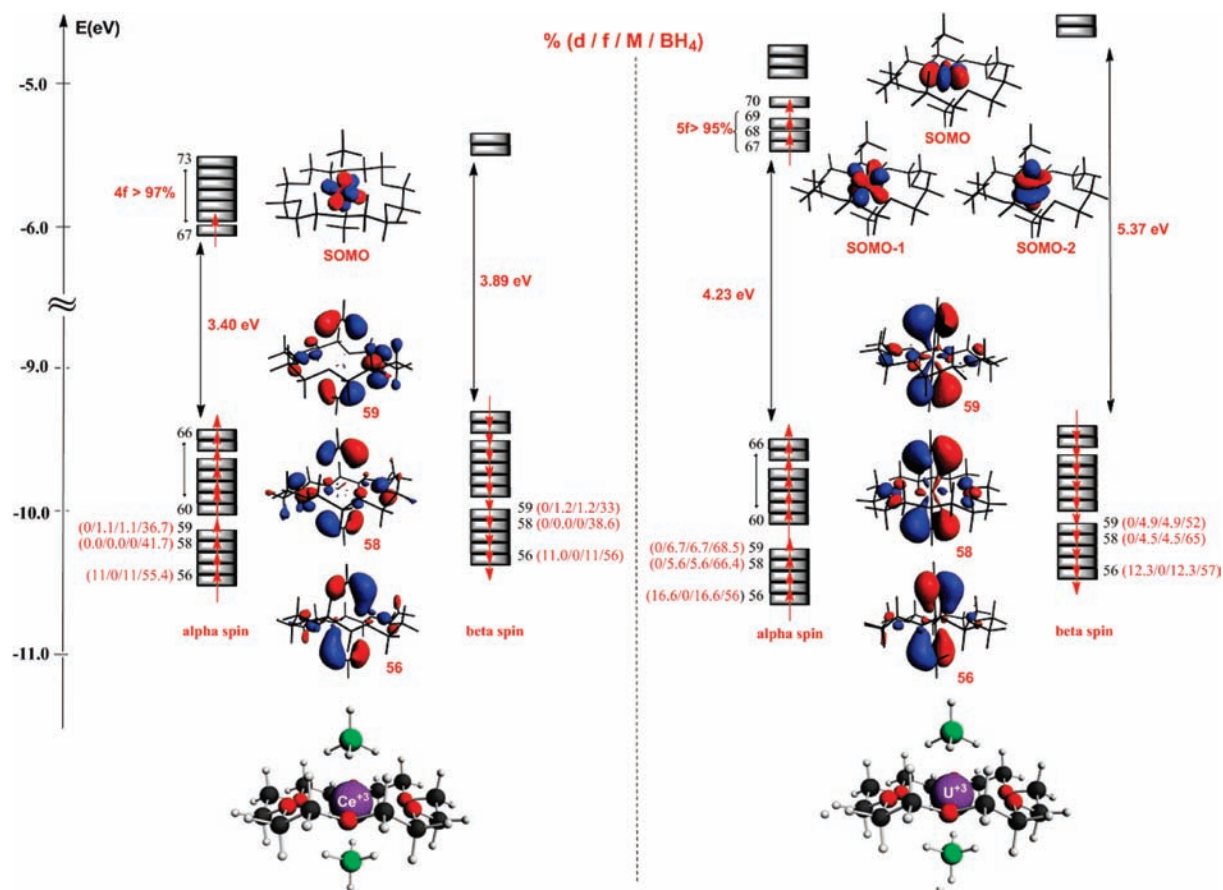


Figure 6. Spin-unrestricted frontier MO diagrams of the Ce(III) and U(III) complexes in their doublet and quartet states, respectively.

Table 6. Mulliken and NBO (NPA) Analysis

structure	metal		ligand				atom-atom overlap population		NPA			
	spin dens.	net charge					M–B	M–(H _b) ₃	M ^q	B ^x	[BH ₄] [−]	H _{u/b}
		ρ _M	M ^q	B ^x	H _{u/b}	[BH ₄] [−]						
Ce(III) (4f ¹)	1.03	+1.99	+0.77	−0.29/−0.32	−0.52	−0.061	+0.073	+2.42	−0.52	−0.88	+0.08/−0.13	
U(III) (5f ³)	3.11	+0.73	+0.87	−0.25/−0.28	+0.25	−0.116	+0.107	+2.01	−0.46	−0.65	+0.08/−0.09	

Molecular Orbital (MO) Analysis. The stronger interaction between the borohydride ligands and the uranium(III) ion through bridging hydrogen atoms according to an η^3 coordination mode could be exalted by the ability of valence 5f orbitals of uranium(III) to participate in covalent bonding, and this raises the question of the role of 5f orbitals in these B–H_b–M three-center two-electron bridging bonds and their influence on the cerium(III)/uranium(III) differentiation. To address these issues, we have performed a molecular orbital analysis with a particular emphasis on these B–H_b–M interactions.

Comparative frontier spin-unrestricted MO diagrams of the Ce(III) complex and U(III) counterpart in their doublet and quartet states, respectively, are displayed in Figure 6. The percentages $\%(d/f/M/BH_4)$ represent the d and f metal orbital contributions to the MOs, as well as the global contribution of the metal center and of the two BH₄ ligands. The diagrams show that there are two important sets of frontier MOs for the Ce(III) and U(III) systems. The highest occupied molecular orbitals, i.e., singly occupied molecular orbital (SOMO, MO # 67) for the former and SOMO, SOMO-1 and SOMO-2 (MOs # 69, 68, and 67) for the latter, are almost 4f or 5f orbitals. As expected from the Mulliken analysis, there is no evidence for metal-to-ligand back-donation effects. The MOs immediately below the SOMOs appear to be rather different in the two compounds; the ligand-to-metal donation is present in the uranium(III) complex and dominates with the MOs # 59, 58, and 56 below SOMO-2 as shown by the percentage composition $\%(d/f/U/BH_4)$. Indeed, these MOs represent the π bonding interactions between the central metal and the three bridging hydrogen atoms with significant 6d and 5f uranium(III) orbital contributions. On the contrary, these MOs in the cerium(III) complex exhibit a much less metallic weight with practically no participation of the 4f orbitals. For example, the $(d/f/M/BH_4)$ percentages are (0/1.1/1.1/36.7) and (0/6.7/6.7/68.5) for the α -MO # 59 in the cerium and uranium compounds, respectively. That an increase in f orbital participation is responsible for the enhancement of covalency in U–X bonds compared to Ln–X bonds was also recently demonstrated by DFT analysis of the complexes $[M\{N(EPR)_2\}_3]$ (M = La, U; E = O, S, Se, Te)^{19c,f} and

$[M(C_5Me_5)(SBT)_3]^-$ (M = La, Ce, Nd, U; SBT = 2-mercapto benzothiazolate).⁹ⁿ Furthermore, the splitting of the 5f block highlights the major participation of these orbitals in the metal–ligand bonding. This synergetic more covalent interaction is obviously unique to the U(III) system, leading to the Ce(III)/U(III) differentiation. It is also noteworthy that the MO diagrams indicate no direct M–B bonding and confirm the fact that this interaction remains mainly electrostatic as indicated by the NBO boron atomic net charges, −0.52 and −0.46 in the cerium and uranium complexes, respectively (Table 6). Moreover MPA indicates an anti-bonding interaction between the metal and boron atoms, the M–B overlap population being more negative for the uranium than for the cerium compound.

Conclusion

The protonolysis reaction of a M–BH₄ bond by means of the acidic ammonium salt NEt₃HBPh₄ proved to be an efficient route to the cationic complexes $[M(BH_4)_2(THF)_5][BPh_4]$ from the neutral precursors $[M(BH_4)_3(THF)_3]$ (M = U, Nd, Ce), further reaction with 18-crown-6 giving the adducts $[M(BH_4)_2(18-crown-6)][BPh_4]$. The DFT analysis of these compounds showed that the M–BH₄ interaction has a more covalent character for M = U than for M = Ce. This Ce(III)/U(III) differentiation revealed that the increase of the covalent contribution to the metal-borohydride bonding is accompanied by variations in the coordination geometry of the BH₄ ligand, that is, the lengthening of the M–H_b bonds, the opening of the H_b–B–H_b angle, in addition to the shortening of the M···B distance. These structural differences, which are, however, too small to be within reach of the X-ray diffraction experiments, are related to the participation of the uranium 5f orbitals to the B–H_b–M three-center two-electron bond, which is much greater than that of the cerium 4f orbitals.

Supporting Information Available: Tables of crystal data, atomic positions and displacement parameters, anisotropic displacement parameters, and bond lengths and bond angles in CIF format. This material is available free of charge via the Internet at <http://pubs.acs.org>.

IC801685V